THE ARCHIVE OF MECHANICAL ENGINEERING

Vol. LV 2008 Number 1

DOI: 10.24425/ame.2008.131612

**Key words:** three-layered annular plate, viscoelastic core, dynamic stability, time-dependent load, finite difference method, finite element method

*DOROTA PAWLUS*

# DYNAMIC STABILITY OF THREE-LAYERED ANNULAR PLATES WITH VISCOELASTIC CORE

Three-layered, annular plate with viscoelastic core is subjected to loads acting in the plane of the plate facings. One formulates the dynamic, stability problem concerning the action of time-dependent compressive stress on a plate with imperfection. This problem has been solved. One created the basic system of differential equations in which the approximation finite difference method was used for calculations. The essential analysis of the problem was concentrated on evaluation of the influence of the plate imperfection rate and the rate of plate loading growth on the results of calculation of critical parameters at the moment of loss of plate stability. It determines the analysed problem of sensitivity of the plate to imperfection and loading. In the evaluation of the dynamics of this problem, the dynamic factor defined as the quotient of the critical, dynamic load to the static one was used. The idea of dynamic factor and the type of the accepted criterion of the loss of plate stability were taken from the Volmir's work. The observations were confirmed by comparable results of calculations of plate models built in finite element method using the ABAQUS system. The analysis of the stress state in an exemplary plate model calculated in FEM demonstrated the importance of the strength condition in total evaluation of the plate work. One achieved satisfactory correctness of results in both methods.

## 1. Introduction

The investigations in the field of the stress-strain analysis of annular plates with laminar transverse structure subjected to the lateral loads are still being undertaken. These investigations consider the plates with different properties of layer material, particularly with damping layer and the plates with different geometrical parameters. The effects of the facing

* *University of Bielsko-Biala, Faculty of Mechanical Engineering and Computer Science, 43-309 Bielsko-Biala, ul. Willowa 2, Poland; E-mail: doro@ath.bielsko.pl*

to core thickness ratio or the radius dimension to total plate thickness ratio are studied. The problems, like e.g.: static and dynamic stability or the vibrations analysis are examined. Certain works concerning these problems, which appeared recently are written by the following authors: Yu and Huang [1], Krizhevsky and Stavsky [2], Paydar [3], Dumir, Joshi and Dube [4], Wang and Chen [5], [6], [7], Chen, Chen and Wang [8]. The evaluation of behaviour of plates analysed in such problems is a multi-parameter complex task.

In the present work, examinations of dynamic stability of annular plates with three-layered structure were undertaken. Especially, the attention was focused on the influence of the plate imperfections and the increase in load parameter on critical plate parameters and its supercritical behaviour. This work is an extension and a complement to the analyses of examined plates presented in work by Pawlus [9], [10], [11]. The form of the basic system of the differential equations, which is the solution to the problem of deflections of three-layered, annular plates with elastic core under compressive loads, has been presented in work [9]. The calculations were carried out using the approximation finite difference method. The evaluation of the critical plate parameters depending on the effect of thickness and material parameters of plate core was the subject of consideration in work [10]. The calculations were carried out using the method presented in [9] and using the finite element method in the ABAQUS system.

Introducing in considerations of the buckling problem the formulae of the viscoelastic core of three-layered plate subjected to a lateral time-dependent load is the stage of the investigations undertaken in present work. The main goal of the considerations is the plate problem of imperfection and loading sensitivity. Each of the analysed plate examples with specific parameters of core material and thickness constitutes a certain individual plate structure, which has its own preliminary deflection and rate of loading growth expressed by the calibrating number and the plate critical, static load. Some observations in this field for plates with elastic core have been indicated in [11]. The analysis of the loading sensitivity of plates were made for fixed value of the rate of loading growth independently of the material and geometrical parameters of plate.

The way to the solutions to the buckling problem, presented in works [9], [10], [11], refers to the solutions obtained for elastic or viscoelastic homogeneous plate described in works by: Wojciech [12], Trombski and Wojciech [13], Pawlus [14], [15], respectively. The analytical formulae of homogeneous plates have been conformed to the laminar structure keeping the way of numeric solution based on the approximation, finite difference method. In work by Pawlus [16] the behaviours of both homogeneous

and laminar plates with viscoelastic properties have been analysed. The calculations have been carried out using the finite element method in ABAQUS system.

In the present work, the study is also supported by the calculations in finite element method using the ABAQUS system. One presents the mesh model of three-layered plate structure with soft, foam, viscoelastic core.

## 2. Problem formulation

The three-layered, annular plate loaded in the plane of the plate facings is the subject of the consideration. The classical, three-layered transverse structure of the plate is composed of elastic, steel facings and a suitably thicker, soft core made of a foam with viscoelastic properties. The outer plate layers are loaded with uniformly distributed compressed stress $p$ proportionally increasing in time $t$ with the velocity $s$. The formula is as follows:

$$p=st \tag{1}$$

where:
p – compressive stress,
s – rate of plate loading growth,
t – time.

The geometry of the analysed plate is expressed by the dimensions of its inner $r_i$ and outer $r_o$ radius, equal thicknesses of facings $h'$, the thickness of core $h_2$ and by the form and the rate of plate preliminary deflection. The scheme of the examined plate is presented in Fig. 1.

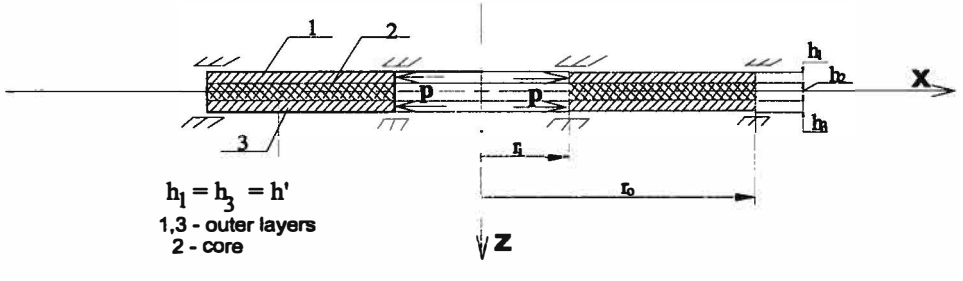


Fig. 1. Scheme of the plate

An axially-symmetrical form of the plate pre-deflection has been accepted in the analysis. This form corresponds with the total axially-symmetrical form of plate buckling. The plate loaded on inner perimeter and supported

in slidably clamped edges is the object of the analysis. The plate loses its stability in this regular form for a minimal value of critical load, important in stability problem. It was observed in static and dynamic stability problem of homogeneous plates [17] and in static stability problem of sandwich plates [18]. The assumed case of plate loading and the form of plate buckling are showed in Fig. 2.

(a) (b)

Fig. 2. Full annulus plate model with the case of loading (a) and the form of axially-symmetrical buckling (b)

The values of critical, dynamic loads denoted in the range of quickly increasing plate deflections in the time of loading strongly depend on both loading velocity and the rate of plate imperfection. The evaluation of the influence of the rate of loading growth $s$ and the imperfection number $\xi$ on the dynamic behaviour of plates with different thicknesses and material parameters of their core is the goal of the undertaken analysis, which could be formulated as the sensitivity of plate to imperfection and loading growth.

The parameter $K_d$, called the dynamic factor in paper [19], is the quantity accepted in the study, which characterizes the plate dynamic stability. Dynamic factor $K_d$ is defined as the quotient of the critical, dynamic load to critical, static one:

$$K_d = \frac{p_{crdyn}}{p_{cr}} \tag{2}$$

The criterion presented by Volmir [19] has been adopted as the criterion of loss of plate stability. According to this criterion, the loss of plate stability occurs at the moment of time when the speed of the point of maximum deflection reaches the first maximum value. This criterion corresponds with the criterion presented by Budiansky-Hutchinson in work [20]. According to this criterion, the critical, dynamic load is the amplitude of the impulse, whose small change

causes the greatest increase in deflections. It was used in the analysis of static and dynamic buckling of laminated composite shells presented by Tanov and Tabiei [21] as the Budiansky-Roth criterion. The criterion presented by Budiansky-Hutchinson is used in work [22] in the problem of dynamic buckling in structures sensitive to imperfection, like: bars, plates and shells.

In the description of rheological properties of the core material, one adopted the formulae of the standard model (Fig. 3) of the linear viscoelastic medium. The transverse deformation of plate core and facings is based on the assumptions of the classical theory of sandwich plates [23] with the broken line hypothesis and the distribution of the plate layers in carrying the stresses: normal stress by the facings, and the shearing one by the core. This scheme of the division of layer loads was used in building the plate computational models:

- in the formulation of the expressions of the basic system of differential equations solving the presented problem with the use of approximation finite difference method;
- in the selection of the mesh elements of the plate models built in finite element method for additional, numeric calculations using the ABAQUS system.

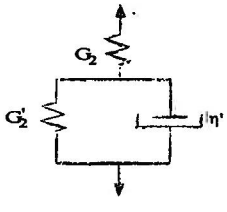


Fig. 3. Standard model

## 3. Basic equations

In formulating the system of differential equations, which solves the plate buckling problem, one assumed equal values of preliminary and additional deflections of each layer. The deformations of the outer layers have been expressed by the nonlinear Kármán's plate equations. The linear physical relations of the Hooke's law and the viscoelastic medium describe the properties of the outer layers and the core, respectively.

### 3.1. Equations of dynamic equilibrium

The system of forces that load the layers of an axially symmetrical, annular sector of a plate is presented in Fig. 4. The equilibrium equations of the plate layers are given by the following formulae:

layer 1

$$\frac{M_{\eta} - M_{\theta_1}}{r} + M_{\eta,r} - Q_{\eta} + \frac{h_1}{2}\tau_{\eta} = 0 \tag{3}$$

$$(r \cdot N_{r_1} \cdot w_{,r})_{,r} + (r \cdot Q_{r_1})_{,r} + r \cdot \tau_{r_1} \cdot w_{,r} = r \cdot h_1 \cdot \mu_1 \cdot w_{,tt} \tag{4}$$

layer 2

$$- Q_{r_2} + \frac{h_2}{2}\tau_{\eta} + \frac{h_2}{2}\tau_{r_3} = 0 \tag{5}$$

$$(r \cdot Q_{r_2})_{,r} - r \cdot \tau_{r_1} \cdot w_{,r} + r \cdot \tau_{r_3} \cdot w_{,r} = r \cdot h_2 \cdot \mu_2 \cdot w_{,tt} \tag{6}$$

layer 3

$$\frac{M_{r_3} - M_{\theta_3}}{r} + M_{r_3,r} - Q_{r_3} + \frac{h_3}{2}\tau_{r_3} = 0 \tag{7}$$

$$(r \cdot N_{r_3} \cdot w_{,r})_{,r} + (r \cdot Q_{r_3})_{,r} - r \cdot \tau_{r_3} \cdot w_{,r} = r \cdot h_3 \cdot \mu_3 \cdot w_{,tt} \tag{8}$$

where:

$M_{\eta(3)}$, $M_{\theta_{1(3)}}$ – elementary, radial and circumferential bending moments of the outer plate layers, respectively,

$Q_{\eta(3)}$, $Q_{r_2}$ – transverse forces on the unit of length of the plate outer layers and the core layer, respectively,

$N_{\eta(3)}$, $N_{\theta_{1(3)}}$ – the normal radial and circumferential forces on the unit of length of the outer plate layers, respectively,

$\tau_{\eta(3)}$ – shearing stress of the outer layers,

r – radius of the plate,

w – plate absolute deflection,

$h_{1(3)}$, $h_2$ ($h_1 = h_3 = h'$) – thickness of the outer layers and the core, respectively,

$\mu_{1(3)}, \mu_2$ ($\mu_1 = \mu_3 = \mu$) – mass density of the outer layers material and the core material, respectively.

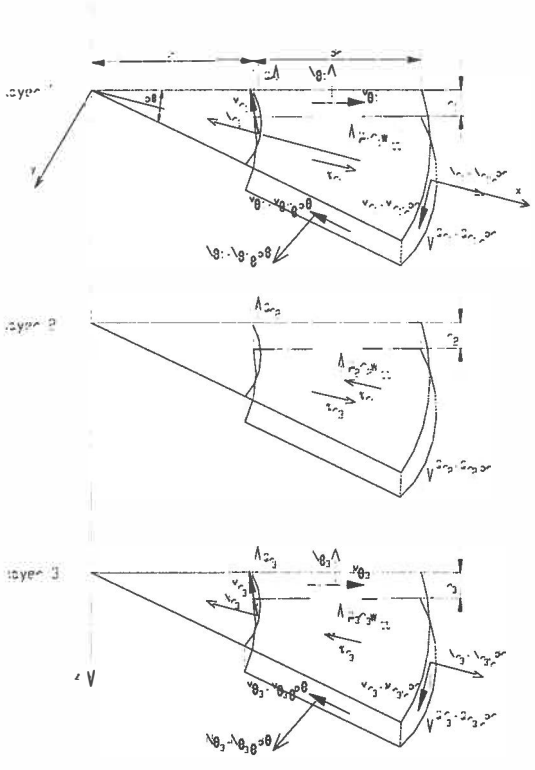

Fig. 4. Loading of layers

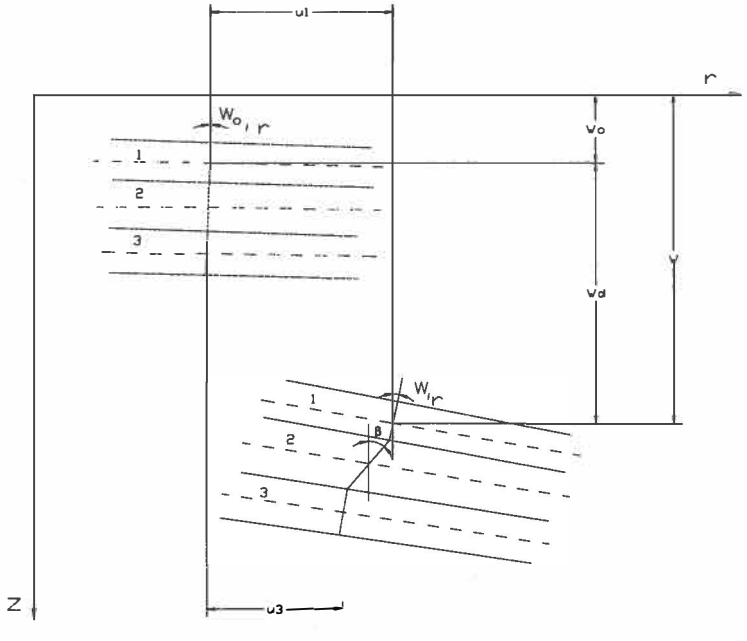


Fig. 5. Cross-sectional plate geometry

### 3.2. Geometric relations

Figure 5 presents the deformation in cross-section structure of the plate. The angle $\beta$ expresses the core deformation, according to the equation:

$$\beta = \frac{u_1 - u_3 - h' w_{d'r}}{h_2} + w_{o_r} \tag{9}$$

where:
$u_1, u_3$ - displacements of the points of the middle plane of the outer layers in the radial direction,
$w_o$ - preliminary deflection,
$w_d$ - additional deflection.

### 3.3. Physical relations

Linear physical relations of the Hooke's law for a plane stress state are expressed as follows:

$$\sigma_{r_i} = \frac{E_i}{1 - \nu_i^2}(\varepsilon_{r_i} + \nu\varepsilon_{\theta_i}) \tag{10}$$

$$\sigma_{\theta_i} = \frac{E_i}{1 - \nu_i^2}(\varepsilon_{\theta_i} + \nu\varepsilon_{r_i}) \tag{11}$$

where:
i - denotes the outer layer, i = 1 or 3.

The values of Young's modulus and Poisson's ratio of the material of the outer layers are equal: $E=E_1=E_3$ and $\nu=\nu_1=\nu_3$ , respectively.

The physical relationship between stresses and displacement in the viscoelastic core material subjected to shearing stress is presented by the equation:

$$\tau_{rz_2} = \tilde{G}_2 \cdot \gamma_{rz_2} \tag{12}$$

where:
$\gamma_{rz_2}$ is the shearing strain of plate core, expressed by:

$$\gamma_{rz_2} = u_{2_z}^{(z)} + w_{d'r} \tag{13}$$

$u_2^{(z)} = u_2 - z\beta + zw_{o_r}$ is the radial displacement of the point in the $z$ distance from of the middle surface of plate core,
$u_2$ - displacement of the points of the middle plane of core layer in the radial direction,

$\tilde{G}_2$ - the modulus expressed by the formula corresponding to the form of constitutive equation of the standard model:

$$\tilde{G}_2\left(\frac{\partial}{\partial t}\right)=\frac{\tilde{A}}{\tilde{B}}=\frac{C+D\frac{\partial}{\partial t}}{E+F\frac{\partial}{\partial t}} \tag{14}$$

C, D, E, F – the quantities formulated by the elastic $G_2$, $G_2'$ and viscosity $\eta$ constants of the core material [24]:

$$C=\frac{G_2G_2'}{G_2+G_2'} \qquad D=\frac{\eta' G_2}{G_2+G_2'} \qquad E=1 \qquad F=\frac{\eta'}{G_2+G_2'} \tag{15}$$

$\frac{\partial}{\partial t}$ - differential operator.

### 3.4. Sectional forces and moments

The relations between sectional forces, moments and stresses in the plate facings are expressed by the force and moments equations in the following form:

$$N_{r_i}=\frac{Eh_i}{1-\nu^2}\left(u_{i,r}+\frac{1}{2}(w_{i,r})^2+\frac{\nu}{r}u_i\right) \tag{16}$$

$$N_{\theta_i}=\frac{Eh_i}{1-\nu^2}\left(\frac{1}{r}u_i+\frac{1}{2}\nu(w_{i,r})^2+\nu\, u_{i,r}\right) \tag{17}$$

$$M_{r_i}=-D\left(w_{d,rr}+\frac{\nu}{r}w_{d,r}\right) \tag{18}$$

$$M_{\theta_i}=-D\left(\frac{1}{r}w_{d,r}+\nu\, w_{d,rr}\right) \tag{19}$$

By using Eqs. (9), (12), (13) one obtains the following form of core transverse force $Q_{r_2}$, determined as $Q_{r_2}=\tau_{rz_2}h_2$:

$$Q_{r_2}=\tilde{G}_2(\delta+H'w_{d,r}) \tag{20}$$

where:
$\delta = u_3 - u_1$, $H' = h' + h_2$.

The resultant, transverse force $Q_r$ has been calculated as the sum of layers forces $Q_{r(2.3)}$ obtained using Eqs. (3), (5), (7). Introducing the expressions presented by the Eqs. (18), (19), (20), after the transformation, one obtains the following form of resultant, transverse force $Q_r$:

$$Q_r = -2Dw_{d'rrr} - \frac{2D}{r}w_{d'rr} + \frac{2D}{r^2}w_{d'r} + \tilde{G}_2\left(\delta + H'w_{d'r}\right)\frac{H'}{h_2} \tag{21}$$

where:

$D = \frac{Eh'^3}{12(1-\nu^2)}$ is the flexural rigidity of the plate facings.

The resultant radial $N_r$ and circumferential forces $N_\theta$ as the sum of the facing forces $N_r = N_{r_1} + N_{r_3}$, $N_\theta = N_{\theta_1} + N_{\theta_3}$ have been determined by the stresses function $\Phi$:

$$N_r = 2h'\frac{1}{r}\Phi_{,r} \tag{22}$$

$$N_\theta = 2h'\Phi_{,rr} \tag{23}$$

### 3.5. Initial conditions

The initial state of the plate determined for additional deflection and its velocity is expressed as follows:

$$w_d\big|_{t=0} = 0 \qquad w_{d't}\big|_{t=0} = 0 \tag{24}$$

### 3.6 Boundary conditions

The conditions of slidably clamped edges are:

$$w\big|_{r=r_0(r_1)} = 0 \qquad w_{,r}\big|_{r=r_0(r_1)} = 0 \qquad \delta\big|_{r=r_0(r_1)} = 0 \qquad \delta_{,r}\big|_{r=r_0(r_1)} = 0 \tag{25}$$

The loading boundary conditions for the radial stresses and their derivatives with respect to time $t$ can be written as follows:

$$\sigma_r\big|_{r=r_1} = -p(t)\cdot d_1 \qquad \sigma_r\big|_{r=r_0} = -p(t)\cdot d_2 \tag{26}$$

$$\sigma_{r_1}|_{r=r_1} = -s \cdot d_1 \quad \sigma_{r_1}|_{r=r_0} = -s \cdot d_2 \tag{27}$$

where:
$d_1$, $d_2$ – determined by the value, equal to 0 or 1 of the loading inner or/and outer plate edges.

### 3.7. Form of predeflection

The assumed form of pre-deflection of axially symmetrical plate presented earlier in [13], [17] is described by the following equation:

$$\varsigma_o(\rho) = \xi(\rho^4 + A_1\rho^2 + A_2\rho^2 \ln\rho + A_3 \ln\rho + A_4) \tag{28}$$

where:
$\xi$ is the calibrating number,
$\varsigma_o = \frac{w_o}{h}$, $\rho = \frac{r}{r_o}$ are the dimensionless values of pre-deflection and plate radius.

### 3.8. Basic system of differential equations

Adding the terms of Eqs. (4), (6), (8) and using Eqs. (21), (22) of radial, resultant forces, one calculates the following form of the differential equation of plate deflections:

$$\begin{aligned}&\tilde{B}k_1 w_{d,rrr} + \tilde{B}\frac{2k_1}{r} w_{d,rr} - \tilde{B}\frac{k_1}{r^2} w_{d,r} + \tilde{B}\frac{k_1}{r^3} w_{d,r} - \tilde{A}\frac{H'^2}{h_2} w_{d,rr} - \tilde{A}\frac{1}{r}\frac{H'^2}{h_2} w_{d,r} + \\ &- \tilde{A}\frac{1}{r}\frac{H'}{h_2}\delta - \tilde{A}\frac{H'}{h_2}\delta_{,r} = \tilde{B}\frac{2h'}{r}(w_{,r}\Phi_{,rr} + \Phi_{,r}w_{,rr}) - \tilde{B}w_{d,rr}M\end{aligned} \tag{29}$$

where:
$k_1 = 2D$, $M = 2h'\mu + h_2\mu_2$

Using Eqs. (16), (17), (22), (23), we obtain the equation of inseparability of the deformations (30) and its time differential form (31):

$$r\Phi_{,rrr} + \Phi_{,rr} - \frac{1}{r}\Phi_{,r} + \frac{1}{2}E(w_{,r})^2 = 0 \tag{30}$$

$$r\Phi_{,rrt} + \Phi_{,rt} - \frac{1}{r}\Phi_{,rt} + Ew_{,r}w_{,rt} = 0 \tag{31}$$

The unknown quantity $\delta$ in Eq. (29) has been calculated from the additional equation (32):

$$k_{2_v} r\delta_{,rr} + k_{2_v}\delta_{,r} - k_{2_v}\frac{1}{r}\delta - 2r\tilde{G}_2\delta - 2r\tilde{G}_2 H' w_{d,r} = 0 \tag{32}$$

where: $k_{2_v} = \frac{Eh'}{1-\nu^2}h_2$.

Eq. (32) was formulated using the differences of the terms of equilibrium equations of projections on the x-directions of forces acting on the undeformed plate facing.

## 4. Problem solution

The following dimensionless quantities and parameters have been used in the solution:

$$F = \frac{\Phi}{h^2 E} \quad t^* = t \cdot K7 \quad \varsigma = \frac{w}{h} \quad \varsigma_1 = \frac{w_d}{h} \quad \bar{\delta} = \frac{\delta}{h} \quad K7 = \frac{s}{p_{cr}}$$

$$K5 = \frac{h'}{h} \quad k_{3_v} = r_0 h_2 M \tag{33}$$

where:
$p_{cr}$ is the critical, static plate load.

Introducing the quantities (33) and replacing the derivatives with respect to $\varrho$ by central, finite differences in discrete points, one transforms Eqs. (29), (30 ), (31), (32) to the forms:

$$\mathbf{P_V U} + \mathbf{Q_V} + \mathbf{PT_V}\dot{\mathbf{U}} + \mathbf{QT_V} - EK7^2 k_{3_v}\frac{b^4}{K5}\ddot{\mathbf{U}} = \frac{FK7^3 b^4 k_{3v}}{K5}\dddot{\mathbf{U}} \tag{34}$$

$$\begin{aligned} \mathbf{FF\,Y} &= \mathbf{UW} \\ \mathbf{FF}\,\dot{\mathbf{Y}} &= \mathbf{U}\dot{\mathbf{W}} \end{aligned} \tag{35}$$

$$\mathbf{ZT_V}\dot{\mathbf{D}} = \mathbf{Z_V D} + \mathbf{VT_V}\dot{\mathbf{U}} + \mathbf{V_V U} \tag{36}$$

where:

$\mathbf{P_V}$, $\mathbf{PT_V}$ – matrixes with elements composed of geometric and material plate parameters and quantity $b$ ($b$-length of the interval in the finite difference method);

$\mathbf{Q_v}$, $\mathbf{QT_v}$ – vectors of the expressions composed of initial deflections, geometric and material parameters, components of stress function, quantity $b$ and coefficient $\delta$;

**FF** – matrix with elements described by ratio $a_i = b/\varrho_i$;

**UW**, $\dot{\mathbf{UW}}$ – vectors of the expressions of initial and additional deflections, components of stress function and their derivatives, ratio $a_i$ and quantity $b$;

$\mathbf{ZT_v}$, $\mathbf{Z_v}$, $\mathbf{VT_v}$, $\mathbf{V_v}$ – matrixes of the components of plate geometry and plate material parameters and quantity $b$;

**U**, **Y**, **D** – vectors expresses by the additional plate deflections, components of stress function and coefficient $\delta$.

The differential Eq. (34) has been solved using the Runge-Kutta's integration method for the initial state of plate. Earlier, one calculated the stress function components of the vector **Y** and the derivatives of stress function of the vector $\dot{\mathbf{Y}}$ from Eqs. (35) and the coefficient $\delta$ and its derivatives as the elements of vectors **D** and $\dot{\mathbf{D}}$, respectively.

## 5. Critical loads of plate with elastic core

The solution to the problem of plate with elastic core requires only the modification of Eqs. (15) to the forms, which correspond to the case of instantaneous elastic deformation, i.e., when $\eta'$ and $G_2'$ are equal to: $\eta'=0$, $G_2' \to \infty$. Then, the values of the quantities C, D, E, F are equal, respectively: E=1, C=G, F=D=0. Eqs. (34), (35), (36) are transformed to the form of equations excluding the additional expressions connected with the existence of the differential operator $\frac{\partial}{\partial t}$. Eq. (34) becomes a differential equation of second order. The system of Eqs. (34), (35), (36) can be written in the form:

$$\mathbf{P_V U} + \mathbf{Q_V} = K7^2 k_{3_v} \frac{b^4}{K5} \ddot{\mathbf{U}} \tag{37}$$

$$\mathbf{FF\,Y} = \mathbf{UW} \tag{38}$$

$$\mathbf{Z_V D} = \mathbf{V_V U} \tag{39}$$

Critical, static stress $p_{cr}$ has been calculated from the Eq. (37) neglecting the inertial components and initial deflection, and assuming the stresses function $F$ as a solution to the disk state. After transformation, Eq. (37) takes the following form:

$$\mathbf{MAP}\cdot\mathbf{U}+\mathbf{MACD}\cdot\mathbf{D}=p^{*}\mathbf{MAC}\cdot\mathbf{U} \tag{40}$$

where:
$p^*$ – dimensionless stress, $p^{*}=\frac{p}{E}$
**MAP, MACD, MAC** – matrices of components of geometric and material plate parameters and quantity $b$.

By solving the eigenproblem, one calculates the minimal value of dimensionless stress $p^*$ as the critical, static load $p_{cr}^{*}$ of plate:

$$\det\left(\left(\mathbf{MAP}+\mathbf{MACD}\cdot\mathbf{Z}_{V}^{-1}\mathbf{V}_{V}\right)-p^{*}\mathbf{MAC}\right)=0 \tag{41}$$

where:
$\mathbf{Z}_V^{-1}$ is the inverse matrix to $\mathbf{Z}_V$ in Eq. (39).

## 6. Exemplary calculations

The exemplary calculations have been carried out for two kinds of polyurethane foams core material:

– with values of constants $G_2$, $G_2'$, $\eta'$, $\mu_2$ presented in work [25] equal to: $G_2$=15.82 MPa, $G_2'$=69.59 MPa, $\eta'=7.93\times10^4$ MPa×s, $\mu_2$=93,6 kg/m$^3$, respectively;

– with the data presented in work [26] for the Kirchhoff"s modulus $G_2$, equal to: $G_2$=5MPa, the creep function $\varphi = 0.845(2 - e^{-0.361} - e^{-0.0361})$ and the mass density $\mu_2$ equal to: $\mu_2$=64 kg/m$^3$.

Creep function presented in work [26] allows for calculating the values of elastic and viscous constants of five-parameters rheological model composed of two Kelvin-Voigt models and the spring element connected in series. Because the solution presented in this paper is for the core material described by the three-parameters, standard model (Fig.3), hence the presented characteristic of function $\varphi$ has been approximated by the function of standard model using in the numeric analysis the following values of constants: $G_2$=5 MPa, $G_2'$=3.13 MPa, $\eta'=212.92\times10^4$ MPa×s, accepted for examined three-layered plate.

The plate facings are made of steel with the parameters: Young's modulus $E=2.1\times10^5$ MPa, Poisson's ratio $\nu$=0.3, mass density $\mu=7.85\times10^3$ kg/m$^3$.

The evaluation of the influence of the imperfection degree on the values of dynamic loads has been analysed for the values of calibrating number $\xi$ (presented by Eq. (28) ) in the range of: $\xi$=0.125÷2. However, the influence of the rate of plate loading growth $s$ has been expressed accepting different

values of parameter *K7*, equal to: K7=10,20,40 1/s, which describes the velocity *s* by the formula: $s=K7\times p_{cr}$ – Eq. (33).

The calculations in finite difference method have been preceded by selection of the number *N* of discrete points from among numbers *N*, equal: N=11, 14, 17, 21, 26. The values of critical. dynamic loads $p_{crdyn}$ of plates with viscoelastic core and values of critical, static loads $p_{cr}$ have been evaluated. The numeric calculations show that the number N=14 allows us to achieve the accuracy up to 5% of technical error. The calculations were carried out for this number. Tables 1, 2, 3 present the exemplary results of the analysis.

Table 1.

Values of critical loads for different values of number *N*

$E=2.1\times10^5$ MPa, $\nu=0.3$, $\mu=7.85\times10^3$ kg/m$^3$, $G_2=5$ MPa
$G_2'=3.13$ MPa, $\eta'=212.92\times10^4$ MPa×s, $\mu_2=64$ kg/m$^3$
$K7=20$ 1/s, $h_2=0.005$ m, $\xi=2$

| $N$ | 11 | 14 | 17 | 21 | 26 |
|---|---|---|---|---|---|
| $p_{crdyn}$ | 78.81 | 79.62 | 79.78 | 80.10 | 80.17 |
| $p_{cr}$ | 74.70 | 75.61 | 76.05 | 76.36 | 76.57 |

Table 2.

Values of critical loads for different values of number *N*

$E=2.1\times10^5$ MPa, $\nu=0.3$, $\mu=7.85\times10^3$ kg/m$^3$, $G_2=15.82$ MPa
$G_2'=69.59$ MPa, $\eta'=7.93\times10^4$ MPa×s, $\mu_2=93{,}6$ kg/m$^3$
$K7=40$ 1/s, $h_2=0.02$ m, $\xi=0.125$

| $N$ | 11 | 14 | 17 | 21 | 26 |
|---|---|---|---|---|---|
| $p_{crdyn}$ | 373.57 | 391.48 | 398.43 | 401.49 | 402.12 |
| $p_{cr}$ | 322.32 | 338.94 | 345.56 | 348.82 | 350.58 |

Table 3.

Values of critical loads for different values of number *N*

$E=2.1\times10^5$ MPa, $\nu=0.3$, $\mu=7.85\times10^3$ kg/m$^3$, $G_2=15.82$ MPa
$G_2'=69.59$ MPa, $\eta'=7.93\times10^4$ MPa×s, $\mu_2=93{,}6$ kg/m$^3$
$K7=20$ 1/s, $h_2=0.005$ m, $\xi=2$

| $N$ | 11 | 14 | 17 | 21 | 26 |
|---|---|---|---|---|---|
| $p_{crdyn}$ | 158.23 | 159.94 | 160.58 | 161.09 | 161.60 |
| $p_{cr}$ | 146.37 | 149.34 | 150.50 | 151.26 | 151.74 |

### 6.1. Plate imperfection sensitivity

The diagrams presented in Figs. 6, 7, 8, 9 show the influence of the values of calibrating number $\xi$ on the time history of plate deflections. The results in Figs. 6, 7 concern the plates with viscoelastic core with elastic constant $G_2$ and thicknesses $h_2$, equal to: $G_2$=5 MPa, $h_2$=0.005 m and 0.02 m, respectively. Figs. 8, 9 show the results of plates with the greater value of elastic constant $G_2$=15.82 MPa of the core material. The analysed plates have been subjected to the load increasing slowly with the velocity expressed by the parameter K7, equal to: K7=10 1/s. The marked point in the curves $\zeta_{1max}=f(t^*)$ determines the critical time and critical deflection at the moment of the loss of plate stability according to the accepted criterion.

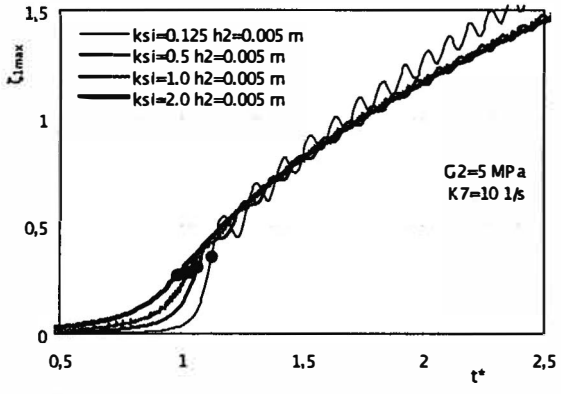


Fig. 6. Time histories of plates with $G_2$=5 MPa and $h_2$=0.005 m for different values of number $\xi$

The presented characteristics show the essential influence of the values of number $\xi$ describing the plate preliminary deflections on the values of dynamic factor $K_d$. The influence is illustrated by the distribution of marked dots in Figs. 6, 7, 8, 9 for plates with different values of material core parameters and core thicknesses. The values of dynamic factor $K_d$ of plates with greater imperfection and plates with thicker core but with lower value of the elastic constant $G_2$=5 MPa approach the value equal to one, or even lower than one. It means that the values of critical, dynamic loads correspond to the values of the critical, static loads or they are lower then static loads. In supercritical area of plate work, one observes the decay of vibrations initiated by the acting load of plates with preliminary deflection scaling greater by the number $\xi$, equal to $\xi$=2.

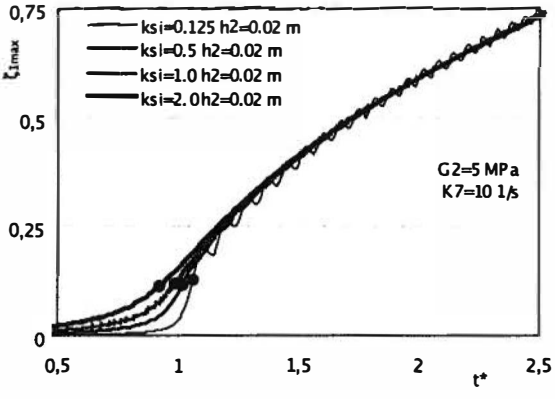


Fig. 7. Time histories of plates with $G_2$=5 MPa and $h_2$=0.02 m for different values of number $\xi$

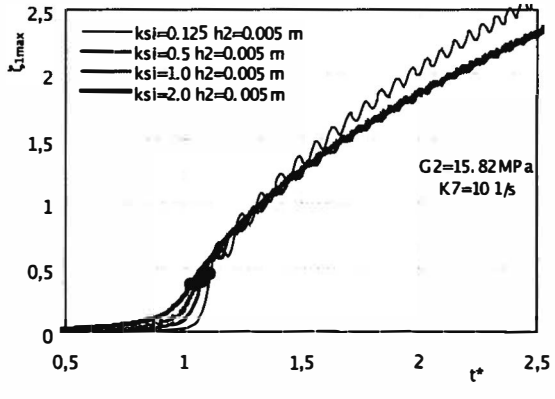


Fig. 8. Time histories of plates with $G_2$=15.82 MPa and $h_2$=0.005 m for different values of number $\xi$

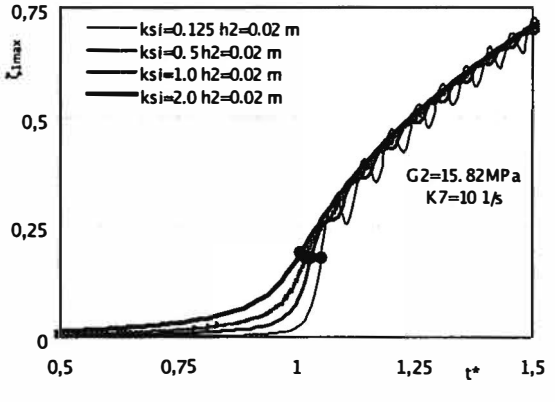


Fig. 9. Time histories of plates with $G_2$=15.82 MPa and $h_2$=0.02 m for different values of number $\xi$

## 6.2. Plate loading growth sensitivity

The influence of the rate of plate loading growth s on plate behaviour is the significant element in its work, too. This influence is depicted by the curves $\zeta_{1max}=f(t^*)$ in Figs. 10, 11, 12, 13 for plates with different core stiffness having the greatest imperfection ($\xi=2$). Then, the dynamic factor $K_d$ of slowly loaded plates is the lowest one, and the values of critical, dynamic loads $p_{crdyn}$ are minimal, too. The values of critical deflections $w_{dcr}$ increase together with the values of the loading growth rate s . Then, the vibrations are initiated by the supercritical, quickly increasing plate loads. They are observed, in particular, for the plates with thinner core ($h_2=0.005$ m).

Table 4.

Values of critical loads depending on the values of number $\xi$ and rate s

| $h_2/G_2$ [m /MPa] | $p_{crdyn}$ [MPa] | | | | | $p_{cr}$ [MPa] | $K_d$ |
|---|---|---|---|---|---|---|---|
| | K7=10 [1/s] | | | K7=20 [1/s] | K7=40 [1/s] | | |
| | $\xi$=0.125 | $\xi$=1 | $\xi$=2 | $\xi$=2 | $\xi$=2 | | |
| 0.005/5.0 | 84.91 | 77.95 | 74.48 | 79.62 | 87.33 | 75.61 | 0.99 |
| 0.005/15.82 | 166.22 | 157.55 | 153.97 | 159.94 | 170.99 | 149.34 | 1.03 |
| 0.02/5.0 | 159.16 | 148.04 | 138.12 | 154.35 | 159.46 | 150.29 | 0.92 |
| 0.02/15.82 | 356.90 | 346.06 | 342.67 | 350.80 | 364.36 | 338.94 | 1.01 |

Table 5.

Values of critical, additional deflections depending on the values of number $\xi$ and rate s

| $h_2/G_2$ [m /MPa] | $w_{dcr}$ [m] | | | | |
|---|---|---|---|---|---|
| | | K7=10 [1/s] | | K7=20 [1/s] | K7=40 [1/s] |
| | $\xi$=0.125 | $\xi$=1 | $\xi$=2 | $\xi$=2 | $\xi$=2 |
| 0.005/5.0 | $2.49 \cdot 10^{-3}$ | $1.99 \cdot 10^{-3}$ | $1.91 \cdot 10^{-3}$ | $2.52 \cdot 10^{-3}$ | $3.25 \cdot 10^{-3}$ |
| 0.005/15.82 | $3.21 \cdot 10^{-3}$ | $2.62 \cdot 10^{-3}$ | $2.60 \cdot 10^{-3}$ | $3.26 \cdot 10^{-3}$ | $4.19 \cdot 10^{-3}$ |
| 0.02/5.0 | $2.84 \cdot 10^{-3}$ | $2.60 \cdot 10^{-3}$ | $2.49 \cdot 10^{-3}$ | $3.80 \cdot 10^{-3}$ | $4.21 \cdot 10^{-3}$ |
| 0.02/15.82 | $3.98 \cdot 10^{-3}$ | $3.96 \cdot 10^{-3}$ | $4.25 \cdot 10^{-3}$ | $5.12 \cdot 10^{-3}$ | $6.21 \cdot 10^{-3}$ |

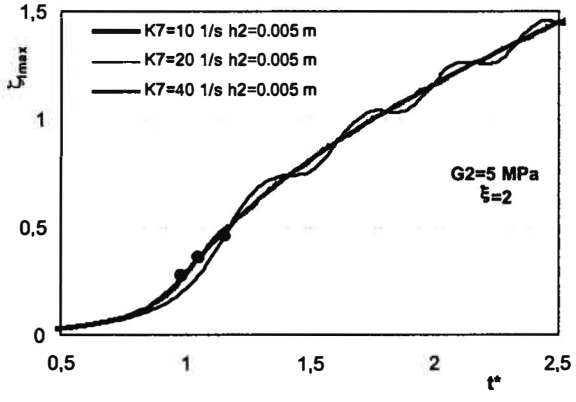


Fig. 10. Time histories of plates with $G_2$=5 MPa and $h_2$=0.005 m for different values of parameter K7

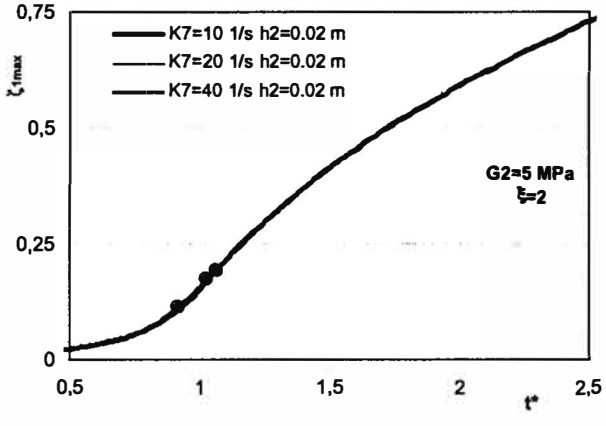


Fig. 11. Time histories of plates with $G_2$=5 MPa and $h_2$=0.02 m for different values of parameter K7

The precise values of critical, dynamic loads $p_{crdyn}$ and critical, additional deflections $w_{dcr}$ for plates with different values of the rate s of plate loading growth are presented in the Tables 4, 5. The critical, additional deflections $w_{dcr}$ in the relation to the absolute plate thickness h are in the range of the 0.27 to 0.6 for plates with thinner core ($h_2$=0.005 m), whereas for plates with thicker core ($h_2$=0.02 m) suitable quotient $w_{dcr}/h$ is in the range from 0.11 to 0.28. According to the accepted criterion of the plate stability loss, the critical deflections of the analysed three-layered plates are practically in the range of up to a half of the total plate thickness.

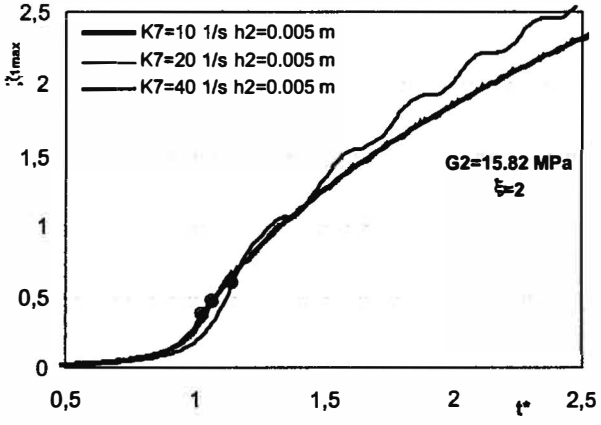


Fig. 12. Time histories of plates with $G_2$=15.82 MPa and $h_2$=0.005 m for different values of parameter K7

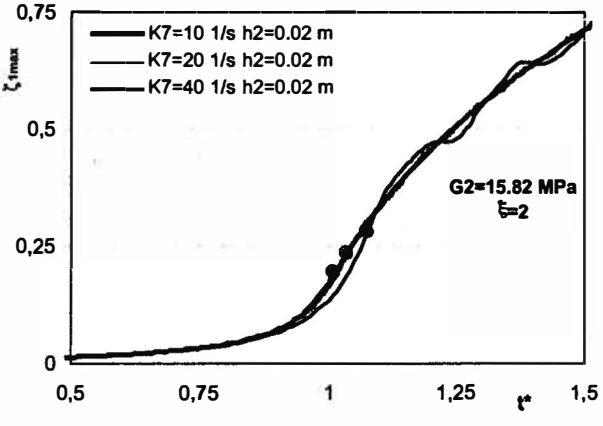


Fig. 13. Time histories of plates with $G_2$=15.82 MPa and $h_2$=0.02 m for different values of parameter K7

## 7. Calculations in Finite Element Method

In order to build the computational mesh for the model of the analysed case of the plate, one applied the simplest solution strategy with the use of axially-symmetric elements. The facings mesh is built of 3-node shell elements, but the core mesh is composed of 8-node solid elements. The schemes of the plate model mesh, the inner loaded model and the axially-symmetrical deformed model are presented in Fig. 14. The outer surfaces of the meshes of facings elements have been tied with the outer surfaces of the core mesh using the surface contact interaction. The conditions of the

slidably clamped edges with a limitation of the possibility of radial, relative displacements of outer layers in plate supports have been introduced. The rate and the shape of preliminary plate deflections correspond to the form accepted for the plate models examined using the finite difference method. The calculations were carried out at the Academic Computer Center CYFRONET-CRACOW (KBN/SGI_ORIGIN_2000/PŁódzka/030/1999) using the ABAQUS system.

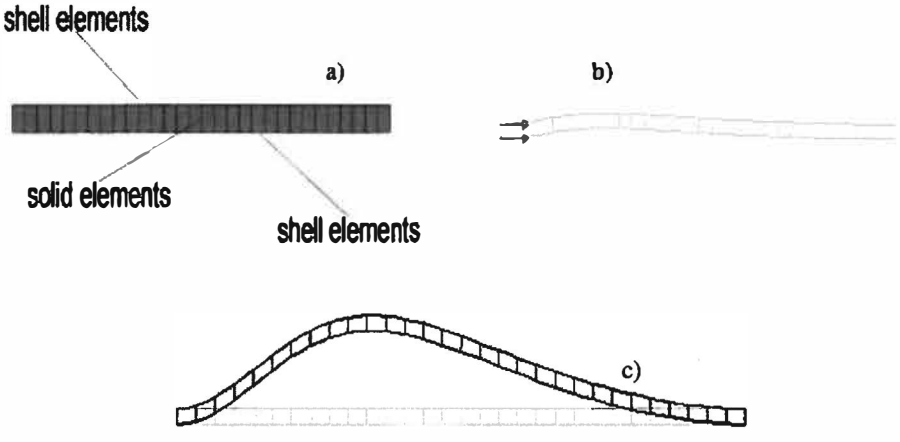


Fig. 14. FEM plate models of : (a) mesh, (b) loading, (c) buckling

In the numerical calculations, the core foam was treated as an isotropic material. One evaluated the values of Young's moduli, equal to: $E_2$=13 MPa and $E_2$=41.13 MPa for the foam material with the values of $G_2$, equal to: $G_2$=5 MPa and $G_2$=15.82 MPa, respectively. According to the standard specification PN-84/B-03230 [27], the value of Poisson's ratio assumed in calculations was $\nu_2$=0.3.

Viscoelastic properties of the core material have been described by a single term of the Prony series for the shear relaxation modulus [28]:

$$G_R(t) = G_o\left(1 - q_1^p\left(1 - e^{-t/\tau_1^G}\right)\right) \tag{42}$$

where:
$q_1^p$, $\tau_1^G$ – material constants,
$G_o$ – instantaneous shear $G_2$.

The values of material constants $q_1^P$, $\tau_1^G$ for the standard model of the plate core have been calculated from the following equations:

$$q_1^P = \frac{G_2}{G_2 + G_2'} \qquad \tau_1^G = \frac{\eta'}{G_2 + G_2'} \tag{43}$$

The results are as follows:
– $q_1^P$=0.615, $\tau_1^G$=26.19×10⁴ s for the foam with $G_2$=5 MPa,
– $q_1^P$=0.185, $\tau_1^G$=928.46 s for the foam with $G_2$=15.82 MPa.

The numerical calculations were carried out for two extreme values of the rate of plate loading growth determined by the parameter *K7*, equal: K7=10 and 40 1/s and for minimal and maximum plate imperfection, i.e. for $\xi$=0.125 and $\xi$=2.

The results of critical loads and deflections are presented in detail in Tables 6, 7. The presented results confirm the observations made for plates calculated using the finite difference method. The minimal values of critical, dynamic loads have been obtained for slowly loaded plates with great imperfection. Then, the values of critical, dynamic loads are slightly lower than the values of critical, static loads, and the values of dynamic factor $K_d$ are lower than 1 irrespective of the analysed plate example. The analysed plate with the stiffest core ($h_2$=0.02 m, $G_2$=15.82 MPa) is the exception in this observation. The value of critical, dynamic load is greater than value of the critical, static one. The obtained values of critical plate deflections are lower than those calculated using the finite difference method.

Table 6.

Values critical loads calculated in FEM depending on the values of number $\xi$ and rate *s*

| $h_2/G_2$ [m /MPa] | $p_{crdyn}$ [MPa] | | | $p_{cr}$ [MPa] | $K_d$ |
|---|---|---|---|---|---|
| | K7=10 [1/s] | | K7=40 [1/s] | | |
| | $\xi$=0.125 | $\xi$=2 | $\xi$=2 | | |
| 0.005/5.0 | 72.32 | 62.72 | 74.24 | 64.0 | 0.98 |
| 0.005/15.82 | 130.71 | 118.72 | 134.31 | 119.92 | 0.99 |
| 0.02/5.0 | 151.79 | 141.77 | 148.93 | 143.20 | 0.99 |
| 0.02/15.82 | 340.02 | 333.7 | 336.97 | 324.01 | 1.03 |

Table 7.

Values of critical deflections calculated in FEM depending on the values of number $\xi$ and rate $s$

| $h_2/G_2$ [m /MPa] | $w_{dcr}$ [m] | | |
|---|---|---|---|
| | K7=10 [1/s] | | K7=40 [1/s] |
| | $\xi$=0.125 | $\xi$=2 | $\xi$=2 |
| 0.005/5.0 | $2.43 \cdot 10^{-3}$ | $1.78 \cdot 10^{-3}$ | $2.98 \cdot 10^{-3}$ |
| 0.005/15.82 | $2.46 \cdot 10^{-3}$ | $2.13 \cdot 10^{-3}$ | $3.49 \cdot 10^{-3}$ |
| 0.02/5.0 | $2.66 \cdot 10^{-3}$ | $3.11 \cdot 10^{-3}$ | $3.62 \cdot 10^{-3}$ |
| 0.02/15.82 | $3.61 \cdot 10^{-3}$ | $4.33 \cdot 10^{-3}$ | $4.42 \cdot 10^{-3}$ |

Figs. 15, 16, 17 present time histories of deflections and velocity of deflections for plates with core parameters: $h_2$=0.005 m, $G_2$=15.82 MPa analysed for the following values: K7=10 1/s, $\xi$=0.125; K7=10 1/s, $\xi$=2; K7=40 1/s, $\xi$=2, respectively. Time histories of deflections for plates with thicker core ($h_2$=0.02 m) and value $G_2$=5 MPa are presented in Fig. 18. The courses of curves illustrating the tendency of rising or decaying of the supercritical vibrations of plates with certain working parameters are perfectly compatible with the results obtained by means of the finite difference method. The FEM calculations make it possible to evaluate the rate of loading of the layers by the analysis of the stress state in the critical area of plate work.

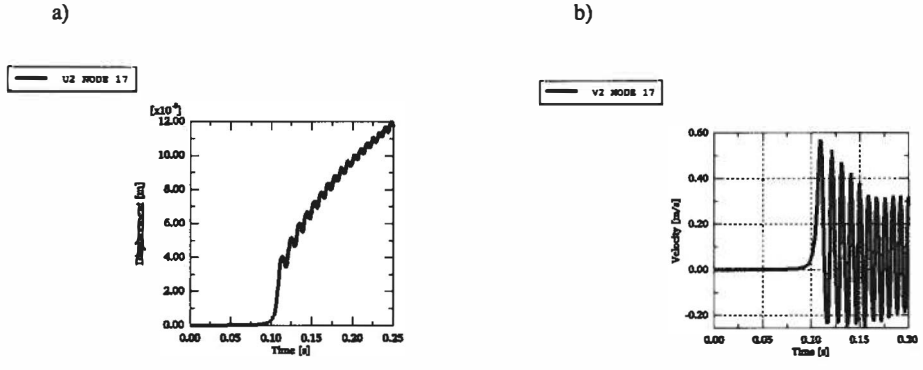


Fig. 15. Time histories of displacements (a) and velocity of displacements (b) for plate with parameters: $G_2$=15.82 MPa, $h_2$=0.005 m, $\xi$=0.125, K7=10 1/s

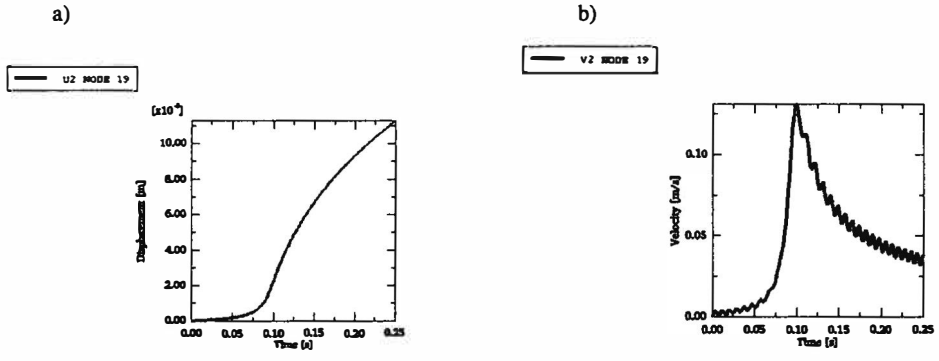


Fig. 16. Time histories of displacements (a) and velocity of displacements (b) for plate with parameters: $G_2$=15.82 MPa, $h_2$=0.005 m, $\xi$=2, K7=10 1/s

The Figs. 19, 20 show the exemplary distributions of equivalent stresses of von Mises type, and core shearing stresses in the *r_z* plane (Fig.5), respectively. The results pertain to the moment of loss of dynamic stability of plate with parameters: $G_2$=15.82 MPa, $h_2$=0.005 m, K7=10 1/s, $\xi$=2. The maximum, critical von Mises stresses in the facing are in the range of 440 MPa, but the critical maximum core shearing stress is about 0.63 MPa. One can notice that the values of stresses are significant. The knowledge about these stresses is important in evaluation of the strength of plate work.

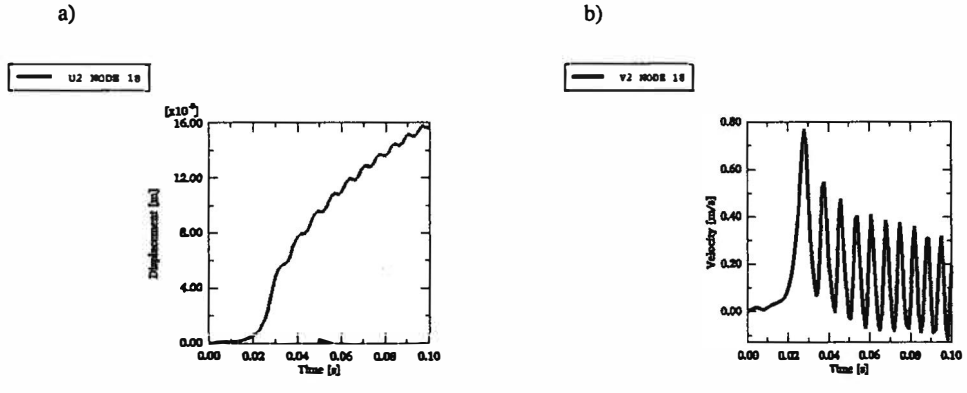


Fig. 17. Time histories of displacements (a) and velocity of displacements (b) for plate with parameters: $G_2$=15.82 MPa, $h_2$=0.005 m, $\xi$=2, K7=40 1/s

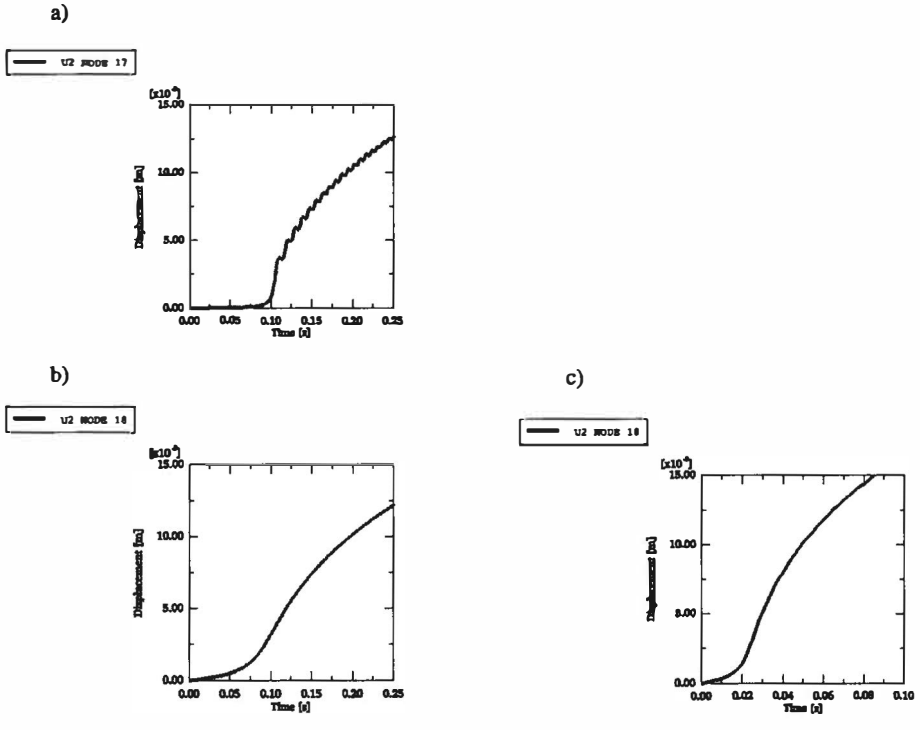


Fig. 18. Time histories of displacements for plate with parameters: $G_2$=5 MPa, $h_2$=0.02 m, (a) $\xi$=0.125, K7=10 1/s (b) $\xi$=2, K7=10 1/s (c) and $\xi$=2, K7=40 1/s

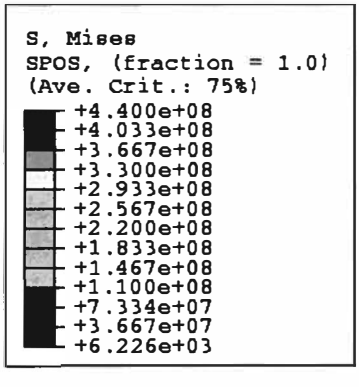


Fig. 19. Distribution of von Mises equivalent stresses in the facing of plate with parameters: $G_2$=15.82 MPa, $h_2$=0.005 m, $\xi$=2, K7=10 1/s

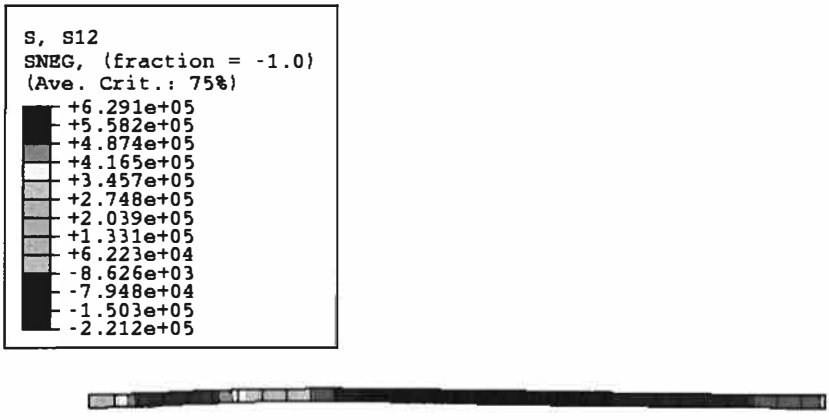


Fig. 20. Distribution of core shearing stresses in the r_z plane for plate with parameters: $G_2$=15.82 MPa, $h_2$=0.005 m, $\xi$=2, K7=10 1/s

## 8. Conclusions

This paper presents a proposal of solution to the buckling problem of three-layered, annular plates with viscoelastic core subjected to a lateral, time-dependent load. The obtained system of differential equations for the analysed plate, applied for calculations in numerical analysis using the finite difference method, is the fundamental element of the solution. The results have been compared with the FEM results of computational plate models. The qualitative consistency and quantitative correspondence have been achieved. The possibilities offered by the finite element method in quick evaluation of the critical stress state for individual plate layers significantly broaden the range of investigations. This evaluation shows the importance of the two analyses, the stability analysis and the strength analysis, for the investigations that have been carried out. The results of the stress state analysis inform about the correctness of using a certain criterion of plate stability loss and essentially limit the supercritical area of plate deflections. It should be noticed that the strength criterion could be the one, which essentially limits the possibilities of plate work. The loading of the analysed plate should be limited to the values, which correspond with the critical, static loads. But for particular plate examples with great imperfection one should realize that the values of critical, dynamic loads are lower than the static ones.

It could be shown that the sensitivity of the analysed plates to geometrical, material and loading parameters is significant. The differences in values of critical, dynamic loads for various numbers $K7$ and $\xi$ are in the range of a

dozen or so MPa, but the values of critical deflections differ by up to 40% of their calculated values.

The evaluation of critical loads of three-layered plates with imperfection is a multi-parameter, complex problem, which requires detailed analysis. The assumption that the form of plate preliminary deflection is different than that which corresponds to the total form of plate buckling could be an essential, additional factor influencing plate stability investigations. The analysis of homogeneous plates [13], [17] indicates that the influence of axially-symmetrical components in the description of the shape of plate preliminary geometry on the final results (i.e. the form of plate buckling and the values of critical parameters) is significant. Such observations concern the plate examples in which the loss of stability takes wavy forms for the minimal values of critical loads. These solutions are expected for such plates as those analysed in this paper, but loaded on their outer perimeter. This problem could be the subject of the future investigations based on general solution of plates with circumferential, wavy forms. Such solutions to the static stability problem of three-layered, annular plates were presented in work by Pawlus [18]. These were also based on the two methods: finite difference and finite element.

Manuscript received by Editorial Board, October 16, 2007;
final version, March 18, 2008.

## REFERENCES

[1] Yu SC, Huang SC.: Vibration of a three-layered viscoelastic sandwich circular plate. *International Journal of Mechanical Sciences* 2001; 43: pp. 2215÷2236.
[2] Krizhevsky G, Stavsky Y.: Refined theory for vibrations and buckling of laminated isotropic annular plates. *International Journal of Mechanical Sciences* 1996; 38(5): pp. 539÷555.
[3] Paydar N.: Axisymmetric buckling of an annular sandwich plate of varying thickness. *Composite Structures* 1990; 15: pp. 149÷159.
[4] Dumir PC, Joshi S, Dube GP.: Geometrically nonlinear axisymmetric analysis of thick laminated annular plate using FSDT. *Composites: Part B* 2001; 32: pp. 1÷10.
[5] Wang HJ, Chen LW.: Vibration and damping analysis of a three-layered composite annular plate with a viscoelastic mid-layer. *Composite Structures* 2002; 58: pp. 563÷570.
[6] Wang HJ, Chen LW.: Axisymmetric dynamic stability of sandwich circular plates. *Composite Structures* 2003; 59: pp. 99÷107.
[7] Wang HJ, Chen LW.: Axisymmetric dynamic stability of rotating sandwich circular plates. *Journal of Vibration and Acoustics* 2004; 126: pp. 407÷415.
[8] Chen YR, Chen LW, Wang CC.: Axisymmetric dynamic instability of rotating polar orthotropic sandwich annular plates with a constrained damping layer. *Composite Structures* 2006; 73(2): pp. 290÷302.
[9] Pawlus D.: Calculations of three-layered annular plates under lateral loads. *Studia Geotechnica et Mechanica* 2003; XXV(3-4): pp. 89÷109.

[10] Pawlus D.: Dynamic stability problem of three-layered annular plate under lateral time-dependent load. *Journal of Theoretical and Applied Mechanics 2005*; 43(2): pp. 385÷403.
[11] Pawlus D.: Critical loading of three-layered annular. Proceedings of the International Colloquium of IASS Polish Chapter on Lightweight Structures in Civil Engineering, Warsaw, Poland, 12–14 September 2005, pp. 308÷313.
[12] Wojciech S.: Numeryczne rozwiązanie zagadnienia stateczności dynamicznej płyt pierścieniowych. *Journal of Theoretical and Applied Mechanics* 1979; 2(17): pp. 247÷262.
[13] Trombski M, Wojciech S.: Płyta pierścieniowa o ortotropii cylindrycznej obciążona w swej płaszczyźnie ciśnieniem zmiennym w czasie. *The Archive of Mechanical Engineering* 1981; XXVII (2): pp. 161÷181.
[14] Pawlus D.: The behaviour of ring-shaped viscoelastic plate. Proceedings of the International Colloquium of IASS Polish Chapter on Lightweight Structures in Civil Engineering, Warsaw, Poland, 30 November–4 December 1998, pp. 152÷157.
[15] Pawlus D.: Numerical solutions of deflections of linear viscoelastic annular plates under lateral variable loads. *Machine Dynamics Problems* 2000; 24(3): pp. 93÷112.
[16] Pawlus D.: Homogeneous and sandwich elastic and viscoelastic annular plates under lateral variable loads. Proceedings of the Third International Conference on Thin-Walled Structures, Elsevier Science, 2001, pp. 515÷522.
[17] Wojciech S.: Stateczność dynamiczna ortotropowej płyty pierścieniowej obciążonej w swej płaszczyźnie ciśnieniem zmiennym w czasie. Ph.D. Thesis, Politechnika Łódzka, 1978.
[18] Pawlus D.: Solution to the static stability problem of three-layered annular plates with a soft core. *Journal of Theoretical and Applied Mechanics* 2006; 44(2): pp. 299÷322.
[19] Volmir C.: Nonlinear dynamic of plates and shells. Science, Moskwa 1972, (in Russian).
[20] Hutchinson JW, Budiansky B.: Dynamic buckling estimates. AIAA Journal 1966; 4–3: pp. 525÷530.
[21] Tanov R, Tabiei A.: Static and Dynamic Buckling of Laminated Composite Shells. Proceedings of the 5-th International LS-DYNA Users Conference, South Field, MI, Sept. 1998.
[22] Gryboś R.: Stateczność konstrukcji pod obciążeniem uderzeniowym. Warszawa–Poznań, PWN, 1980.
[23] Volmir C.: Stability of deformed system. Science, Moskwa 1967, (in Russian).
[24] Skrzypek J.: Plastyczność i pełzanie. Warszawa, PWN 1986.
[25] Romanów F.: Wytrzymałość konstrukcji warstwowych. WSI w Zielonej Górze, 1995.
[26] Majewski S., Maćkowski R.: Pełzanie spienionych tworzyw sztucznych stosowanych jako rdzeń płyt warstwowych. Inżynieria i Budownictwo 1975; 3: pp. 127÷131.
[27] Standard, PN-84/B-03230 Lightweight curtain walls and roofs of sandwich and rib panels. Static calculation and design, (in Polish).
[28] ABAQUS/Standard. User's Manual, version 6.1. Hibbitt, Karlsson and Sorensen, Inc. 2000.

## Stateczność dynamiczna pierścieniowych płyt trójwarstwowych z rdzeniem lepkosprężystym

Streszczenie

W pracy przedstawiono rozwiązanie zagadnienia stateczności dynamicznej pierścieniowej płyty trójwarstwowej z miękkim, lepkosprężystym rdzeniem. Rozważaniom poddano

przypadek płyty dwustronnie utwierdzonej przesuwnie, o symetrycznej strukturze poprzecznej, ściskanej na wewnętrznym brzegu jej okładzin liniowo narastającym w czasie obciążeniem. W przedstawionym rozwiązaniu zagadnienia wykorzystano dwie metody: metodę różnic skończonych i metodę elementów skończonych. Metodę różnic skończonych zastosowano w wyprowadzeniu i numerycznym rozwiązaniu postaci podstawowego układu równań różniczkowych (34), (35), (36) analizowanej płyty z rdzeniem lepkosprężystym. Obliczenia metodą elementów skończonych prowadzono wykorzystując system ABAQUS dla przedstawionego w pracy modelu badanej płyty. Otrzymane dwoma metodami wyniki numerycznych obliczeń porównano uzyskując dobrą ich zgodność. W analizie problemu szczególną uwagę zwrócono na wpływ stopnia ugięcia wstępnego i prędkość obciążania analizowanej płyty na wartości krytycznych jej parametrów wyznaczonych w momencie utraty stateczności dynamicznej płyty. W wyznaczeniu utraty dynamicznej stateczności płyty przyjęto kryterium przedstawione w pracy [23]. W ocenie prezentowanych wyników dynamicznych i statycznych obciążeń krytycznych wykorzystano współczynnik dynamiczny $K_d$ będący ilorazem tych wielkości. Obserwowane znaczące różnice wartości dynamicznych obciążeń krytycznych płyt o różnym stopniu ich wygięcia wstępnego i zmiennej prędkości obciążania wskazały na istotną imperfekcyjną i obciążeniową wrażliwość badanej płyty i ważny udział obu badany parametrów w ocenie wyników końcowych. Wykorzystując metodę elementów skończonych wyniki uzupełniono analizą stanu naprężeń krytycznych wyznaczonych w momencie utraty stateczności płyty.